PARTICLE ENHANCED ACTIVE COOLING CONTROL SYSTEM WITHOUT PUMPING PENALTY

José L. Lage

Mechanical Engng. Dep., Southern Methodist University, Dallas-TX 75275-0337

Amir Kiaee

Design Engineer, Applied Materials, Santa Clara-CA 95054

ABSTRACT

Active cooling control systems usually consist of a liquid flowing through regular heated channels. These systems have limited thermal efficiency mainly because boundary layers grow along the channel surfaces, hindering the heat transfer to the moving fluid. Alternative designs, such as turbulators, oscillators, mixers, and fluid enhancers (e.g., nanofluids), can alleviate this hindering "breaking" the boundary layers but at the expense of substantially increased pumping power. The search for a system capable of enhancing the convective heat transfer without increasing the pumping power led us to the unique new cooling system considered here. This system uses a heterogeneous solid-fluid medium consisting of solid particles, of size similar to the channel size, flowing with the liquid. As this medium flows through a heated channel, the particles act locally as pistons essentially pushing the boundary layers downstream of the channel, leaving behind a fresh, undeveloped flow section. Results obtained using start-up numerical simulations of a single particle flowing through a heated isothermal channel show the heat flow from the channel surface to increase by over 30% as compared to the cooling without the particle. Surprisingly, and because the particle flows freely with the moving liquid, there is essentially no pressure-drop increase in the system (> 1%), hence with essentially no pumping power penalty, making this a transformative new cooling control system.

NOMENCLATURE

a	acceleration vector [m/s^2]
D	particle diameter [m]
F	force vector [N]
H	channel dimension [m]
HF	average heat flux over the channel length [W/m^2]
k	fluid thermal conductivity [W/m K]
L	channel length [m]
L_d	developing length, 0.05HRe, [m]
L_i	initial particle location [m]
m	mass [kg]
P	pressure [Pa]
Pr	Prandtl Number, ν/α

q"   heat flux [W/m^2]

Re   Reynold number, U_iH/ν

t   time [s]

T_i initial fluid and particle temperature and at the channel inlet [K]

T_w channel surface temperature [K]

u   velocity vector [m/s]

U_i fluid velocity at the channel inlet [m/s]

U_{max} clear fully developed maximum fluid velocity [m/s]

x   longitudinal channel coordinate [m]

y   transverse channel coordinate [m]

Symbols

α thermal diffusivity [m^2/s]

δ gap distance between channel surface and particle (m)

η_{HF} clear-to-particle heat transfer improvement (%)

ν momentum diffusivity [m^2/s]

ρ density [kg/m^3]

τ scaled time, $t[U_i/(U_{max})]$, [s]

INTRODUCTION

Thermal engineers continuously look for ways to increase heat transfer in heat exchangers with minimum cost. There are several active and passive techniques one can pursue for achieving high convective heat transfer in channel flows, including the use of actuators, geometric changes, surface roughness and solid obstacles to induce mixing and disrupt the boundary layers that otherwise form and hinder heat transfer along the channel[1-3]. All these methods have one thing in common: the action to improve the heat transfer is based on "breaking" the boundary layer along the channel surfaces, which leads to an undesired by-product, i.e., the dramatic increase in the pressure-drop along the channel. The increase in pressure-drop, in turn, yields the need for more pumping power (higher cost) to maintain the fluid flowing.

A more modern alternative to obtain higher heat transfer is based on particulate flows, a class of multiphase (solid-fluid) flows with a very large number of very small particles (usually nanoparticles), all dispersed in the fluid medium forming a slurry. This alternative presents tremendous practical challenges, such as agglomeration of the solid particles, settling, and the usual increased pressure-drop (pumping power).

There is, however, one naturally occurring particulate flow that differs from the slurry flow and is observed in the flow of blood through alveolar capillaries[4], as shown in figure 1. The main characteristic of this flow is the dimension of the particles (the red cells) being similar to the capillary channel cross-section dimension. Notice the gas exchange process in alveolar capillaries, where red blood cells (RBCs) flow with blood plasma, yield very high gas transfer efficiency. An important characteristic of alveolar capillary blood flow, believed to be related to the high efficiency of the lungs, is the snug fitting of the RBCs into the capillaries[5].
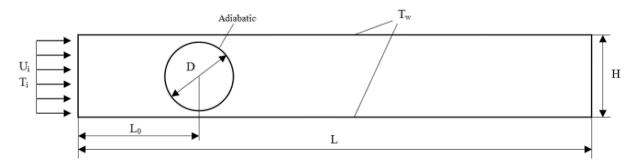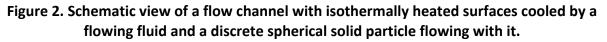
Figure 1. Red blood cells flowing with plasma through a capillary with similar dimension.

The overall objective of the present paper is to present numerical results of convective heat transfer due to a particle flow in heated circular channels where the diameter of the particles is very close to the channel diameter. A similar configuration was considered[6-8] for studying only the flow (no heat transfer) of ice and water through a circular pipe in a train-like fashion.

PROBLEM DESCRIPTION AND MODELING

Focusing on the main characteristic of capillary blood flow, the basic configuration considered in this study is a start-up configuration shown in figure 2, where a straight, finite length channel is filled with an initially isothermal and stationary fluid, containing a solid, neutrally buoyant, adiabatic spherical particle of diameter D, positioned equidistant from the channel surfaces and at a short distance L_0 from the channel inlet. Fluid and particle are initially at the same temperature T_i.

Figure 2. Schematic view of a flow channel with isothermally heated surfaces cooled by a flowing fluid and a discrete spherical solid particle flowing with it.

At a certain time, the surfaces of the channel are set at a temperature T_w higher than the fluid and particle initial temperature T_i, and the fluid (and particle) are set to move by imposing a constant and uniform fluid speed U_i at the channel inlet.

The ensuing transient convection process that follows can be modelled numerically by solving the balance equations for the fluid and solid particle, with boundary and coupling conditions (i.e., equal temperature and heat flux) at their interface. The basic continuity, momentum, and energy equations for a Newtonian fluid with constant and uniform properties are respectively:

$$\nabla . \mathbf{u} = 0 \tag{1}$$

$$\frac{\partial \mathbf{u}}{\partial t} + (\mathbf{u} . \nabla) \mathbf{u} = -\frac{1}{\rho} \nabla P + \nu \nabla^2 \mathbf{u} \tag{2}$$

$$\frac{\partial \mathrm{T}}{\partial t} + (\mathbf{u} . \nabla) \mathrm{T} = \alpha \nabla^2 \mathrm{T} \tag{3}$$

The momentum balance equation for the solid particle, assumed neutrally buoyant and rigid (i.e., non-deformable) is the Newton second law $\mathbf{F} = m\mathbf{a}$, where $\mathbf{F}$ is the force imposed by the flowing liquid, and m and $\mathbf{a}$ are the mass and acceleration of the particle.

The Immersed Solids method is used here to simulate numerically the convection process through the channel. The method involves the use of an immersed solid domain placed inside the fluid domain. The balance equations for fluid and particles are solved using a second-order accurate finite volume method, with cell vertex domain discretization, and the simplified one-way FSI procedure for the momentum equation - note the particle is not allowed to rotate or oscillate, and is considered rigid, neutrally buoyant, imposing an obstruction to the flowing fluid in the form of viscous and form resistance, which then drives the particle via action-reaction effect. A clear (of particle) case, in which the particle is absent from the channel flow, is also simulated numerically for comparison, being the base-line case to which the performance of the flow with the particle is compared. Hexahedral stationary mesh with 152,000 fluid cells for the clear case and about 19,200 cells for the particle is used, for being determined to offer a good compromise between the required computational time for convergence and grid independence. Time step size was chosen as 0.01 s based on time step independency studies.

The following numerical results are for the case of L = 200 mm, L_0 = 12 mm, H = 4.8 mm, and T_i = 300 K. Considering the fluid as water, Pr = 6.13, and the inlet fluid speed U_i = 2.5, 5, 10, 17, and 26 mm/s, the corresponding range of Reynolds number, defined in respect to H and U_i, would be $27 \leq Re \leq 280$. The developing length for the clear flow L_d = 0.05 H Re, would then vary as $6.5 \text{ mm} \leq L_d \leq 67.2 \text{ mm}$, which is much smaller than the channel length. This ensures a developed flow at the exit of the channel, making the presence of the particle likely more effective to improve the convection process. At the channel outlet, the pressure is set as P = 0 (equivalent to a fully developed flow condition) and $\partial T/\partial x = 0$. The channel surface temperature at time zero of the simulation is T_w = 340 K (constant and uniform). Finally, two

distinct particle diameters are considered, namely for D = 4 and 2 mm. Observe the large
diameter allows for only a 0.4 mm gap spacing between the particle and the channel surfaces.

RESULTS

Results for the large and small particle cases with inlet speed U_i = 0.026 m/s (Re = 280) are
shown in figure 3. From top to bottom the figure shows three sets of the time evolution of the
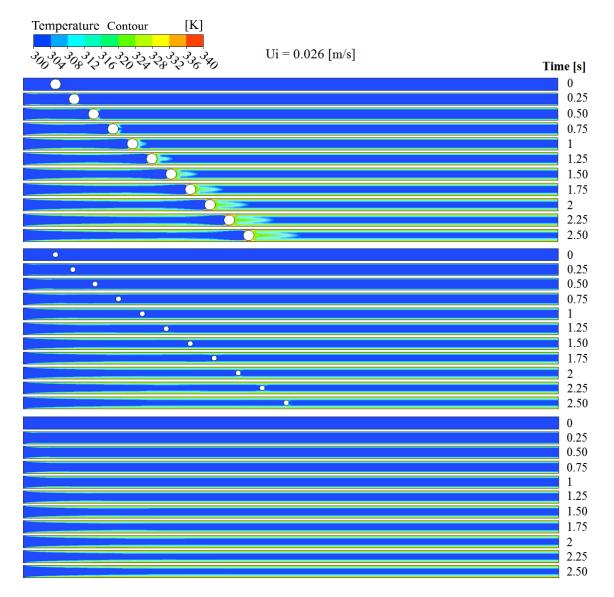convection process with large (top), small (middle), and no particle (bottom).

Figure 3. Convection time evolution with a large particle (D = 4 mm, top), a small particle (D = 2 mm, middle), and a clear fluid (bottom), with inlet velocity 0.026 m/s.

Two effects by the large particle are clearly seen as the flow advances, namely the accumulation of warm fluid downstream of the particle, and the pulling (dragging) of cold inlet fluid further into the channel. These effects are not noticeable in the small particle results. Observe also how the small particle flows further downstream of the channel than the large particle at the same time. As both particles are centered in the channel, the small particle moves faster for being surrounded by fluid moving at faster speed, on average, than the large particle.

The speed of the particle flowing with the fluid in the channel can be estimated using the position versus time plot. An example is shown in figure 4, where the position of both, large and small, particles in the channel is plotted versus time. Observe in both cases U_i = 0.026 m/s. The linear relations between position and time shown as dashed lines suggest the constant terminal speed for both, large and small particles, have been achieved within the observed time period. The slopes of the linear curves indicate the large and small particle speeds to be 0.029 m/s and 0.0358 m/s, respectively. For the large particle, an analytical prediction yields a particle speed of 0.028 m/s, which compares very well with the numerical result. It is worth recalling in fully developed flow the maximum velocity U_{max} occurs at the center of the channel and is U_{max} = 1.5 U_i. Hence, with average speed U_i = 0.026 m/s, U_{max} = 0.039 m/s. Observe the small particle has a terminal speed closer to the fully developed clear flow maximum speed than the large diameter particle, as expected.
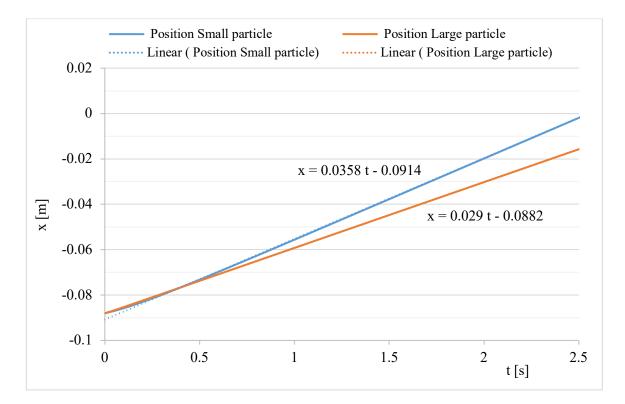

Figure 4. Position of small and large particles versus time with inlet velocity 0.026 m/s.

Figure 5 shows results for U_i = 0.0025 m/s (Re = 27). The average temperature of the fluid in the channel is higher in this case, than the temperature observed in figure 3, because the flow rate is smaller, making the large particle effects more clearly seen.
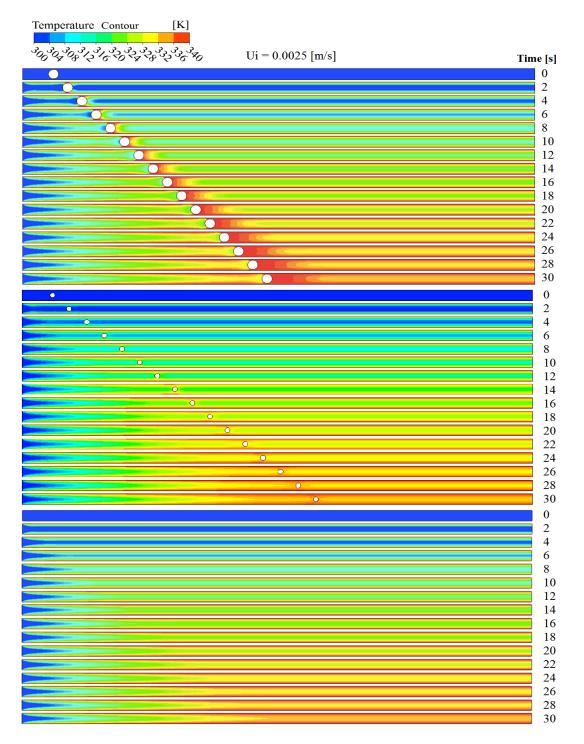

Figure 5. Convection time evolution with a large particle (D = 4 mm, top), a small particle (D = 2 mm, middle), and a clear fluid (bottom), with inlet velocity 0.0025 m/s.
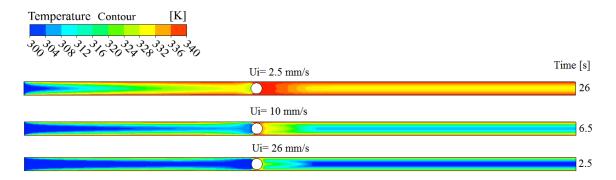
Figure 6. Temperature contours for cases with different U_i and same particle location.

Figure 6 compares the resulting temperature distributions inside the channel for cases with three distinct U_i and for the particle at the same location along the channel (and, of course, at different times). The top channel result, for the case of the smallest inlet flow speed U_i = 0.0025 m/s, has the shortest developing length of all three cases. Interestingly, the fluid immediately downstream of the particle seems to be in thermal equilibrium with the channel surface within the entire channel cross section. This shows the effect of the particle to push, or sweep, downstream the heated fluid accumulated along the channel wall. The fluid isotherms in this region have a concave C-pattern with the highest temperature near the channel surface. This means the heat transfer process from the channel surface is ineffective in this region. As the inlet speed increases (from top to bottom channels in figure 6), however, the isotherms concavity of this region switches to a convex pattern, with the warm fluid now located toward the center of the channel. The cooler fluid near the channel surface would lead to a more effective convection heat transfer there.

At the upstream (left side) of the particle, no matter how high the inlet velocity is, there is always a relatively low temperature fluid bulk trailing the particle, which causes lower mean temperature and enhances the heat transfer from the channel surfaces. Hence, the presence of the particle causes two different heat transfer effects: downstream of the particle the concentration of warm fluid may increase or decrease the heat transfer depending on temperature distribution – concavity; and, upstream of the particle the dragged cold fluid should always increase locally the convection heat transfer from the channel surfaces. The overall improvement of using the particle will certainly depend on these two effects.

The results presented so far clearly indicate the heat transfer improvement by the particle sweeping effect depends on the particle size and the inlet flow speed. The results of figures 3 and 5 show a very weak effect when using the small particle; hence the focus now turns to the large particle case. The local, instantaneous effect of the flowing particle is better identified in figure 7, where the calculated heat flux transferred from the channel surfaces to the fluid, namely $q'' = -k\, \partial T/\partial y$, is plotted along the channel surface at six different times for U_i = 0.026 m/s. The dashed lines show the resulting heat flux for the clear fluid case, for reference. Keep in mind the heat flux is infinite at the starting of the flow for all cases.
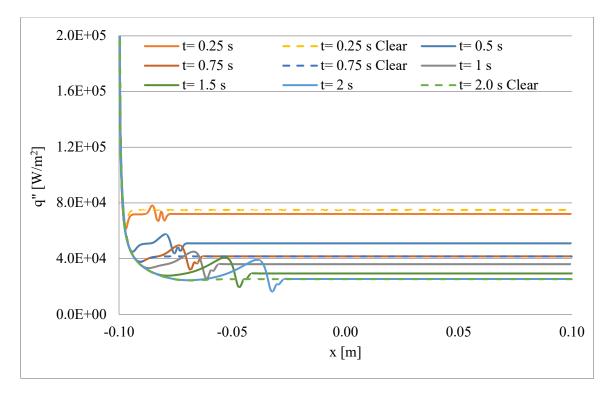
Figure 7. Variation of the heat flux along the channel for the large particle (continuous lines) and clear flow (no particle, dashed lines) cases, with U_i = 0.026 m/s.

After the initial precipitous q" drop near the inlet, the curves for the clear cases (dashed lines) recover a little and settle rapidly to a constant value for the rest of the channel. Notice the recovery in the q" curves for the clear case tend to die out as time goes by (no longer visible when t = 2 s). The curves for the particle case match the initial q" drop and recovery near the inlet and depart from the clear case curves showing a pronounce fluctuation constrained within a region of particle influence. This region stretches during the flow, achieving a size of about 1-2 particle diameters of increased q" (in relation to the clear flow) downstream of the particle and about 8-10 particle diameters of depressed q" upstream of it (see t = 2 s). After achieving a minimum within the depression region, q" recovers to the clear flow value beyond which the two curves become identical. The region with q" above the clear flow case seems comparatively bigger than the region with q" below it. Hence, it seems the heat flux increase upstream the particle predominates over the heat transfer decrease downstream the particle.

To quantify the overall particle effect on the heat transfer along the channel, Figure 8 shows again both curves, for clear flow and particle cases, at time 2 s. Because the heat fluxes are different only in the particle region of influence, with the two cases matching precisely everywhere else within the channel, the difference in the total heat transfer between the clear flow and the particle cases is the difference between the two shaded areas shown under each curve in figure 8. Note the two vertical lines included in the figure are to clearly show the region of particle influence in this case.
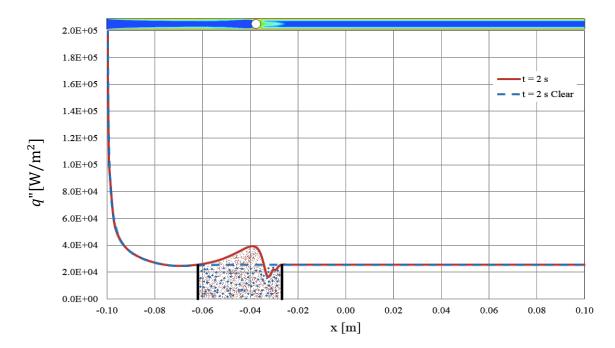
Figure 8. Local difference between heat flux along the channel for clear fluid and particle cases at time 2 s, with large particle and inlet speed of 0.026 m/s.

The areas of these regions yield the total heat flow for each case and can be calculated using numerical integration. Let HF_P and HF_C be the results for the particle and the clear flow cases, respectively. A figure-of-merit of the particle heat flow effect, is defined as:

$$\eta_{HF} = \frac{HF_P - HF_C}{HF_C} \times 100 \quad\quad (4)$$

where η_{HF} is the percent variation of HF_P in relation to HF_C.

The result of calculating η_{HF} for the entire period of the flow is shown in figure 9, for the large particle case and distinct inlet velocities varying from 0.0025 m/s to 0.026 m/s. The horizontal axis of figure 9 is a *scaled time* τ = t $[U_i/(U_{max})]$, introduced to allow for presenting all curves, each for a different U_i, with the same time axis range. Most curves clearly show a very large enhancing effect on the convection heat transfer by the presence of the particle. The curve for U_i = 0.0025 m/s (Re = 27) stands out as being the only case in which no improvement is observed during the entire flow period. The hindering of the heat flow by the particle in the case of low flow speed (because of the hot fluid accumulation downstream of the particle) has been mentioned already in conjunction with figure 6. This suggests for a certain channel width, particle size and thermal conditions, there might be a minimum flow speed for which the particle enhances the heat transfer process. From the results of figure 9, this inlet speed seems to be around 0.010 m/s.
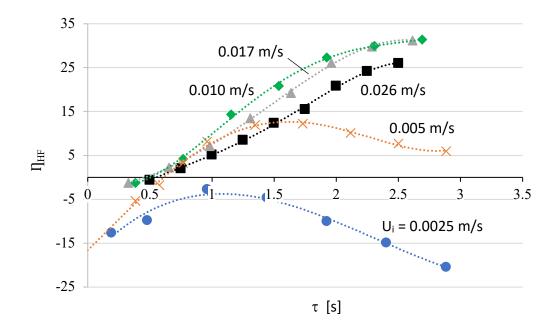
Figure 9. Time variation of percentage heat flux difference between the particle and clear flow cases for a large particle (D = 4 mm) and different inlet speed U_i using a scaled time.

The general pattern of all curves in figure 9 is for η_{HF} to increase to a maximum value and then decrease with a slower rate as time goes by. High inlet speed yield η_{HF} curves with high peaks, and the peaks tend to occur at later τ values, as one would expect (because of the high flow speed). Obviously, if the flow speed is too high, the peak may fall outside the channel; in other words, the channel is not long enough for the convection process to benefit entirely from the fast-moving particle. That is why an optimum speed exists.

It has been mentioned previously the main purpose of having a particle flowing with the fluid in a heated channel is to dislodge the boundary layers leading to an enhanced convection process. Hence, one can infer the particle must reach the boundary layers to be effective. Considering the boundary layers always grow from the surfaces of the channel toward the center of the flow, an effective particle flowing with the fluid should then get very close to the channel surfaces, and that is why large (in relation to the channel size) particles are best. One needs to be very careful with this conclusion: as the particle size increases, the distance between the moving particle and the stationary channel surface decreases. Because the particle flows as a solid in the channel, the fluid velocity distribution within the gap between the particle and the channel surfaces is likely to increase to maintain the same cross section mass flow along the channel. From one side, this fluid velocity increase in the gap is good for helping the local convection effect (faster fluid near the channel surface enhances the heat transfer). Also, this analysis answers why a particle is likely more effective in enhancing convection when used in laminar flow – turbulent flows already present high fluid speed near the channel surfaces, making the speed increase by the particle in this region less impactful. Notwithstanding, the increase speed can yield another undesired effect: an increased shear stress along the channel

surface, inevitably leading to higher pump power to sustain the particle flow. If this happens, one might return to the initial dilemma of having a way to enhance the heat transfer process but at a high pumping power cost.

To investigate the effect of the particle on the flow near the channel surface, figure 10 shows a series of fluid velocity profiles on different cross sections of the channel, drawn at the same time. The profiles are upstream, downstream and around a solid spherical particle that flows with the fluid. Notice this configuration is one in which the flow is laminar, and the fluid velocity has achieved a fully developed profile upstream and downstream of the particle (the leftmost and rightmost velocities profiles show the flow is not affected by the particle in these regions), a case for which the particle would be most effective in enhancing the heat transfer from the channel surfaces.

The average longitudinal fluid speed in figure 10 is U_{ave} = 0.010 m/s and the maximum velocity is U_{max} = 0.015 m/s, which occurs at the center of the channel when the flow is in the fully developed condition. As one progresses visually from upstream (left) to downstream (right) of the particle, the parabolic fully developed velocity profile flattens in the center of the channel as the particle is approached. With the fluid speed getting slower in the center channel region, the fluid must speed up closer to the channel surfaces to compensate and maintain mass conservation in every cross section of the channel (steady flow and incompressible fluid); this is observed by a slight deformation in the velocity distribution of the 3rd profile (from the left) near the gap region.
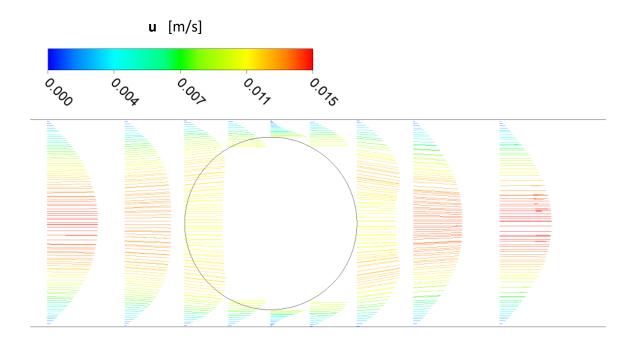

Figure 10. instantaneous fluid velocity vector distribution at different cross sections located upstream, downstream and at the particle location along the channel.

The third profile from the left demarcates the last profile outside the particle from upstream. The next profile to the right does not show the velocity distribution in the region occupied by the particle, because that region has a uniform speed – the particle speed. Observe, nevertheless, how the flow velocity distribution within the gap formed by the channel surface and the particle surface (4th, 5th and 6th profiles) increases as one moves to the right in the figure. At the 5th profile, right at the center of the particle, the smallest gap is achieved, and the fluid achieves its highest speed. From that cross section on, the velocity profiles rebuild themselves all to way back to the fully developed profile, achieved at the right most 9th profile in the figure. One final observation: see how the profile tangential to the particle upstream (3rd profile) show the fluid velocities inclining toward the channel surface, as if opening to flow around the particle, and the profile downstream (7th profile) show the fluid velocities inclining toward the center of the channel, as if closing around the particle.

Figure 11 shows a bird's-eye-view of what happens in the gap region by overlapping the fluid velocity profile with the particle (the profile is limited between the channel surface and the particle surface) and without the particle (i.e., the fully developed profile). Using the known velocity distribution equation for fully developed laminar flow one can find the fluid velocity at a distance from the channel surface equal to the gap distance (here, δ = 4 mm); the result is u(δ) = 0.00458 m/s, the location of which is indicated in the figure by the upward arrow. The particle speed in the present case equals 0.01113 m/s, which is equal to the fluid speed tangent to the particle (no slip condition).
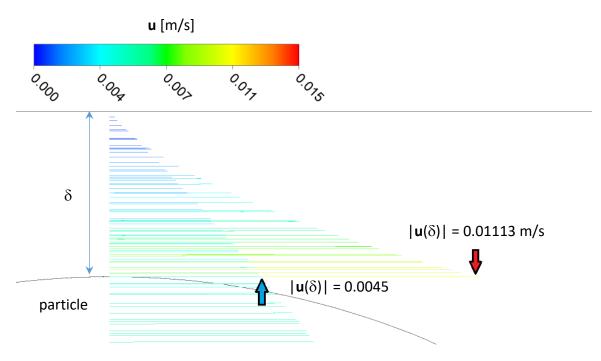

Figure 11. Overlap of the fully developed profile and the velocity profile at the gap between the particle and the channel upper surface.

Hence, the maximum fluid speed at the gap is a whopping 2.43 times greater than the fluid speed at the same location if the particle were not there. Evidently, this fluid speed increase enhances the heat transfer along the channel surface as the particle flows along the channel. Surprisingly, the results indicate a less than 1% increase in the pumping power necessary for maintaining the fluid and the particle flowing in all cases considered here. Although there is a shear stress increase in the gap region, this increase is irrelevant when compared to the total shear stress along the entire channel. The result is a situation in which the convection heat transfer is enhanced, but without any substantial increase in pumping power. Keep in mind the flowing of the particle within the channel is "lubricated" by the thin fluid layer ever present at the gap. Hence, the irrelevant increase in pumping power should not be a surprising result.

SUMMARY AND CONCLUSIONS

Results are obtained via numerical simulations of start-up flow of cooling water along a straight isothermal channel with and without a single solid, adiabatic, neutrally buoyant particle flowing with the fluid. Different fluid speeds and two particle diameters are considered. The results indicate a very small effect by the small particle, particularly when the particle does not reach the boundary layer region growing along the channel surface. This observation led the study to focus on the large particle. Another observed issue is an increased flow speed in laminar flow leads to a stronger convection enhancement by the particle; however, the resulting increase in entrance length will eventually limit the overall particle effect. That is, the results and analysis showed the existence of an optimum fluid speed for enhancing the convection process with a particle. Finally, the particle affects the heat transfer process with enhanced heat transfer upstream the particle location and hindered heat transfer downstream of the particle location as compared to the result obtained for the clear (of particle) flow case. It so happens the enhancement is superior form the hindering, and the introduction of a figure of merit allows the determination of a predominant overall heat transfer enhancement. Although these effects are limited to a flow region around the particle, it is nevertheless substantial, particularly for the case of a large diameter particle when the heat flux increase along the entire channel was shown to reach over 30%.

ACKNOWLEDGEMENT

CONTACT

Dr. Lage is a professor of Mechanical Engineering at the Lyle School of Engineering of Southern Methodist University in Dallas, Texas. A Texas PE, he is the founder of the Thermal Transport Processes Laboratory at SMU, with research funded by the NSF, NIST, and DOE among others.

He was the Associate Chair of the ME Dep, and the President of the SMU Faculty Senate. He has over 200 publications (over 5,000 citations and h = 35) and one patent. Lage is a Pi Tau Sigma Honorary Member, an ASME Fellow, and a member of the ICHMT Scientific Council. He is the recipient of several awards, including the Sigma Xi for Outstanding Research, the ASEE for Outstanding Teaching, and the SMU Golden Mustang. He has been a Visiting Professor of the ETH-Zurich, and of the UTF-PR-Brazil.

REFERENCES

1. Ali Beskok, Mehrdad Raisee, Bayram Celik, Bedri Yagiz, Mohsen Cheraghi "Heat transfer enhancement in a straight channel via a rotationally oscillating adiabatic cylinder" International Journal of Heat and Mass Transfer 58 (2012) 61–69

2. Julian Marschewski, Raphael Brechbühler, Stefan Jung, Patrick Ruch, Bruno Michel, Dimos Poulikakos "Significant heat transfer enhancement in microchannels with herringbone-inspired microstructures" International Journal of Heat and Mass Transfer 95 (2016) 755–764

3. Mark E Steinke, Satish G. Kandlikar "Review of single-phase heat transfer enhancement techniques for application in microchannels, mini-channels and microdevices" International Journal of Heat and Technology 22.2 (2004): 3-11

4. Image from www.slideshare.net Author: the law of science

5. Deniz Ulusarslan, Ismail Teke "An experimental investigation of the capsule velocity, concentration rate and the spacing between the capsules for spherical capsule train flow in a horizontal circular pipe" Powder technology 159.1 (2005): 27-34

6. Deniz Ulusarslan, Ismail Teke "An experimental determination of pressure drops in the flow of low density spherical capsule train inside horizontal pipes" Experimental thermal and fluid science 30.3 (2006): 233-241

7. Ismail Teke, Deniz Ulusarslan "Mathematical expression of pressure gradient in the flow of spherical capsules less dense than water" International journal of multiphase flow 33.6 (2007): 658-674

8. Ali Merrikh, José L. Lage "Effect of Blood Flow on Gas Transport in a Pulmonary Capillary" ASME. *J Biomech Eng.* 2004;127(3):432-439